NJC

Conformational Properties of Aromatic Multilayered and Helical Oligoureas and Oligoguanidines

Journal:	*New Journal of Chemistry*
Manuscript ID:	NJ-FOC-10-2014-001885.R1
Article Type:	Focus
Date Submitted by the Author:	19-Dec-2014

Complete List of Authors:	Kudo, Mayumi; Ochanomizu University, Department of Chemistry, Faculty of Science Tanatani, Aya; Ochanomizu University, Department of Chemistry, Faculty of Science

NJC

RSCPublishing

Focus

Conformational Properties of Aromatic Multi-layered and Helical Oligoureas and Oligoguanidines

Cite this: DOI: 10.1039/c3njoooooox

Mayumi Kudo and Aya Tanatani

Received ooth XXXXX 2013,
Accepted ooth XXXXX 2013

DOI: 10.1039/c3njoooooox

www.rsc.org/njc

The use of *N,N'*-dialkylation of aromatic ureas and guanidines to achieve consecutive stereochemical switching from (*trans,trans*) to (*cis,cis*) conformations provides an elegant methodology for constructing ladder-like multi-layered aromatic oligoureas and oligoguanidines. Here, we highlight the structural properties and functions of these stable, flexible oligomers, which are candidate backbone structures for novel functional materials including electronic devices, chiral recognition, and bioactive substances.

1. Introduction

Foldamers with dynamic conformational properties and functions have potential for mimicking biological macromolecules, such as nucleic acids and proteins, due to their helical or sheet-like structures.[1] In addition, aromatic multi-layered foldamers with longitudinal π-stacked conformations have potential applications in electronic devices. Various multi-layered structures have been reported,[2] for example, based on rigid covalent bonds,[2a] supramolecular assembly via electron donor-acceptor interactions,[2b] and metal coordination networks.[2c] But, because these structures are fixed by covalent bonds or strong interactions, the scope for developing functionality based on dynamic conformational properties is limited.

We have previously reported the unique conformational properties of aromatic amides[3] and their application to construct foldamers.[4] Thus, secondary aromatic amides such as benzanilide exist in *trans* form both in the crystal and in solution, whereas their *N*-methylated compounds exist in *cis* form in the crystals and predominantly in *cis* form in solution (Figure 1a).[3] This phenomenon can be utilized in polymer chemistry; for example, polyamides containing secondary amide bonds with *trans* form generate rod-like sheet structures, while *N*-alkylated polyamides, such as *N*-alkylated poly(*p*-benzamide)s, adopt helical structures driven by the *cis*-conformational preference of *N*-alkylated aromatic amide bonds.[5]

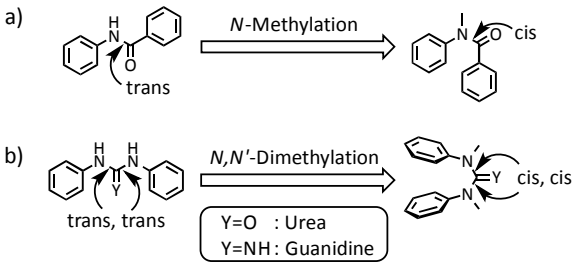

Figure 1. Cis conformational preference of *N*-methylated a) amide, b) urea, and guanidine.

Cis-conformational preference following *N*-alkylation is also observed in aromatic ureas and guanidines, that is, *N,N'*-dimethyl-*N,N'*-diphenylureas and *N,N'*-dimethyl-*N,N'*-diphenylguanidines exist in (*cis,cis*) form, where the two phenyl rings lie in a face-to-face position with a dihedral angle (~30°) smaller than that of *N*-methylbenzanilide (~60°) (Figure 1b), which, amazingly, allows one to construct large aromatic multi-layered molecular structures.[3c,6] These multi-decked structures of *N*-alkylated oligoureas and oligoguanidines are based only on the *cis* conformational preference, and no special interactions, such as hydrogen bonding or metal coordination, are involved. This means that these types of aromatic multi-layers offer a wide range of possibilities for derivatization and applications.

Here, we cast a spotlight on multi-layered aromatic ureas and guanidines generated by utilizing *N*-alkylation-driven *cis*-conformational preference, focusing mainly on fundamental structural analysis and evaluation of biological activities.

2. Structural properties of multi-layered aromatic oligoureas and oligoguanidines

2.1 Structural properties of symmetrical aromatic oligoureas and oligoguanidines

The first example of a multi-layered oligourea was tetra(*p*-phenylurea) (**1**) (Figure 2), which adopts a five-layered structure both in the crystal and in solution.[6a] In the crystal of **1**,

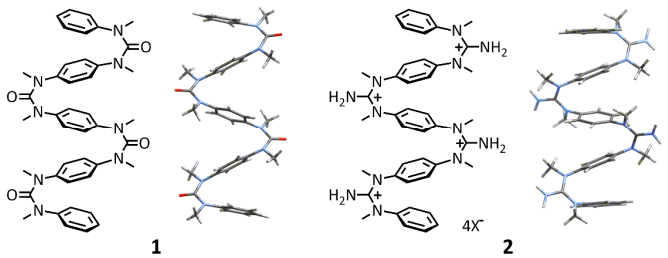

Figure 2. Crystal structures of tetra(*p*-phenylurea) (**1**) and tetra(*p*-phenylguanidine) (**2**).

the dihedral angle between the first and second benzene rings is 38.5° and that between the second and third rings is 46.7°; thus, the angle between the first and the third benzene rings is 12.1°, so that they are close to parallel, with a separation distance of 7.29Å. The crystal structure of tetra(*p*-phenylguanidine) (**2**) closely resembles that of **1**, except for the dihedral angle between the alternate benzene rings (25°).[3c] The solution structures of **1** and **2** are quite similar to the crystal structures, as ascertained by means of ^{1}H NMR studies. The signals of the aromatic protons appear at higher magnetic field (6.4-7.2 ppm) than those of unfolded ureas and guanidines due to ring current effects within the layered structure.

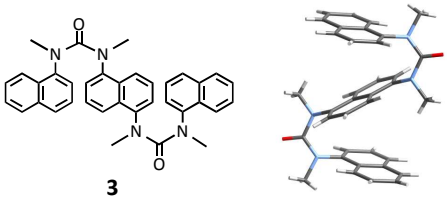

Figure 3. Crystal structure of di(1,5-naphthylurea) (**3**).

The features of (*cis*,*cis*)-ureas can also be observed in di(1,5-naphthylurea) (**3**), as shown in Figure 3; that is, the bis-*cis* conformation of the ureido structure of **3** is retained even with the naphthylenyl groups.[6a] Jørgensen et al reported that a di(1,5-naphthylurea) derivative bearing *N*-benzyl groups (**4**) adopts three different conformers in solution based on rotation around the C-N bond between the naphthalene and urea units (Figure 4).[7] This was clearly observed in variable-temperature (from 300 to 420 K) ^{1}H NMR studies, which showed that the broad signals of naphthalene units become sharper and better defined with increasing temperature due to rapid interconversion between the structures in solution at high temperature. In addition, the crystal structure of **4** includes two possible conformers **4a** and **4c** in the asymmetric unit, which supports two possible types of face-to-face geometry between the naphthalene units.

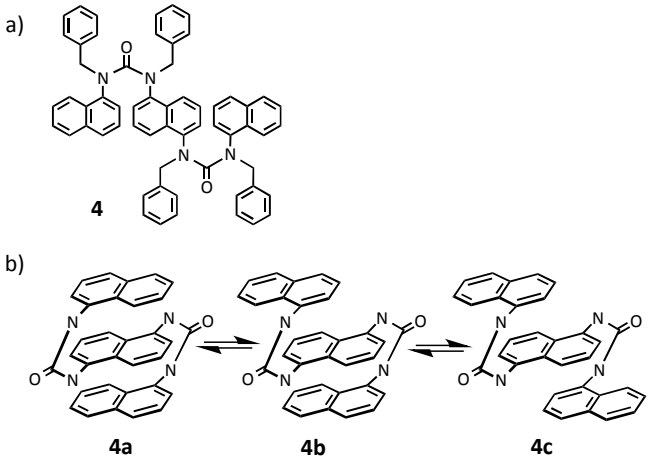

Figure 4. a) Chemical structure of di(1,5-naphthylurea) derivative (**4**). b) Schematic representation of three conformers of (*cis,cis*)-**4**. *N*-Benzyl groups are omitted.

As well as the *para*-linked oligomers, *meta*-linked oligomers also adopt multi-layered structures.[6c] The crystal structures of tetra(*m*-phenylurea) (**5**) and tetra(*m*-phenyl-guanidine) (**6**) are shown in Figure 5a. Both show multi-layered

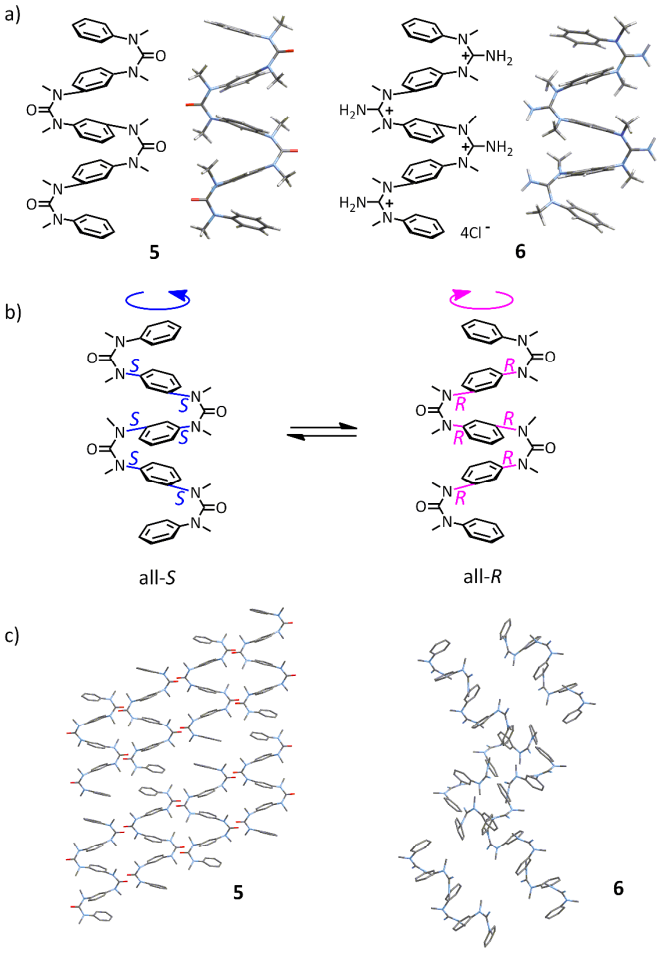

Figure 5. a) Crystal structures of tetra(*m*-phenylurea) (**5**) and tetra(*m*-phenylguanidine) (**6**) The counter anions are omitted. b) Two enantiomeric helical conformations of tetra(*m*-phenylurea) (**5**) with all-*R* or all-*S* axis chirality. c) Packing structures of **5** and **6**.[6c]

aromatic structures with dihedral angles between the two neighboring benzene rings of 30-40° and with the alternate benzene rings being nearly parallel. The distinctive feature of *para*-linked oligomers is the helical structure derived from the identically directed conformations of the two substituents on the benzene rings to form all-*R* or all-*S* axis chirality (Figure 5b). This molecular chirality arises for steric reasons: the well-ordered structures are favored over the diastereomerically broken helical conformations. In the crystal structures of **5** and **6**, the two enantiomeric helices (all-*R* and all-*S*) exist in 1:1 ratio. Interestingly, quite different packing motifs are observed in **5** and **6** (Figure 5c), that is, **5** is ordered in the same direction with an alternate arrangement of all-*R* and all-*S* conformers, and the terminal phenyl groups of one molecule lie in parallel to those of neighboring molecules with the opposite helicity, while **6** forms double zig-zag chains consisting of molecules with the same helicity arranged alternately in reverse directions, and the terminal phenyl groups of two neighboring molecules in one chain form tilted T-shaped structures.[6c] The layered structures of **5** and **6** seem to be retained even in solution, because ^{1}H NMR analyses showed high-field chemical shifts of the aromatic protons, while there is a rapid conversion between the enantiomeric helices (see Section 3).

2.2 Structural properties of unsymmetrical aromatic oligoureas

Lewis et al investigated the structural properties of unsymmetrical oligoureas bearing 1-naphthylenyl and 4-nitrophenyl end groups bridged by either one (**7**) or two (**8**) phenylene diamine units, which could be prototypes for donor-bridge-acceptor systems (Figure 6).[8] Di- and triureas **7** and **8** were efficiently synthesized by converting diarylurea bearing 4-nitrophenyl and 4-aminophenyl groups to the isocyanate, followed by reaction with the corresponding amine and *N*-methylation. The structures of **7** and **8** were predicted by means of Hartree-Fock semiempirical AM 1 calculations to be folded all-*cis* structures, 7 and 17 kcal/mol more stable than the extended structures, respectively, and the predicted structures were supported by the results of solution ^{1}H NMR analyses. The UV absorption and phosphorescence data of **7** and **8** are summarized in Table 1. Both ureas display long-wavelength bands with maxima at 342 nm and strong, long-lived structured phosphorescence at 77K. However, they show no fluorescence, which means the lowest-energy singlet and triplet states are localized on the nitrophenyl chromophore.

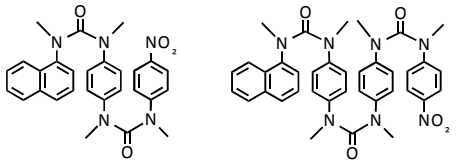

Figure 6. Chemical structures of unsymmetrical di- (**7**) and triurea (**8**).

Table 1. UV absorption and phosphoresence data of **7** and **8**

urea	Absorption (298 K; MTHF solution)		Phosphorescence (77 K; glassy MTHF)		
	λ_{max} (nm)	Log ε	$\lambda_{0,0}$ (nm)	Φ	τ (s)
7	342	4.1	493	0.16	1.25
8	342	4.1	492	0.18	1.32

2.3 Efficient synthetic methodologies of aromatic oligoureas

Conventional synthetic procedures for aromatic layered oligoureas involve multiple condensations, but the overall yield is generally poor because of the large number of reaction steps and the problems of purification at each step.

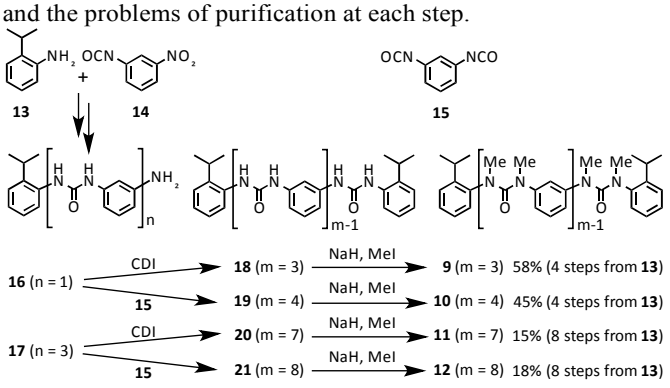

Scheme 1. Efficient synthetic method of symmetrical oligoureas

Clayden et al proposed an elegant synthetic approach to both symmetrical and unsymmetrical oligo(*m*-arylurea)s with various chain lengths.[9] The synthetic strategy involves consecutive elongation of aromatic secondary ureas by repeated condensation, followed by concurrent alkylation of all nitrogen atoms of the ureas to furnish the multi-layered structures. For example, symmetrical oligoureas (triurea **9**, tetraurea **10**, heptaurea **11**, and octaurea **12**) were synthesized by linking together anilines **16** or **17** using carbonyl diimidazole or *meta*-phenylene diisocyanate (**15**), followed by concurrent *N*-methylation (Scheme 1). Unsymmetrical oligo-ureas (diurea **22**, triurea **23**, and tetraurea **24**) were synthesized by hydrogenation of the nitro group of ureas **27**, **28** and **29** prepared by iterative cycles of condensation and hydrogenation, followed by condensation with the terminal aryl isocyanate and *N*-methylation (Scheme 2). In both cases, only a single column-chromatographic purification is required after the *N*-methylation, which is convenient, and improves the overall yield.

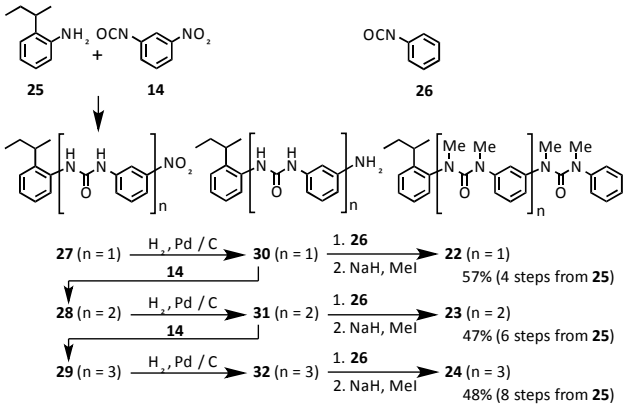

Scheme 2. Efficient synthetic method of unsymmetrical oligoureas

2.4 Cocrystals of aromatic oligoureas with melamine

Since the urea linkers in the layered structures can be regarded as supports of the aromatic moieties, furnishing columns of aromatics, it may be possible to change the shape of these columns by utilizing supramolecular interactions.

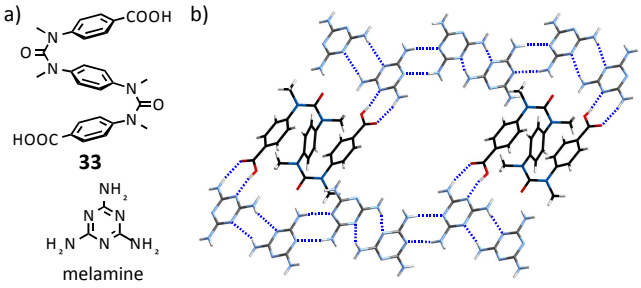

Figure 7. a) Chemical structures of phenylenediurea dibenzoic acid (**33**) and melamine. b) Crystal structure of **1**·(melamine)$_2$·ethyl acetate·DMF showing the network of H-bonds (blue). For clarity, solvated ethyl acetate and DMF molecules are omitted.

Kohmoto et al investigated the cocrystal structures of phenylenediurea-dibenzoic acids (**33**) (Figure 7a) with melamine molecules.[10] In the cocrystals, **33** possesses meso-conformation, driven by the opposite directions of twisting of the first and second urea linkers, and is packed with melamine in an interpenetrating fishnet-type structure derived from the zig-zag pattern of the melamine network (Figure 7b). This

network consists of three cyclic H-bonding motifs: two of them are between neighboring melamine molecules, and the other involves the adjacent carboxy group. A possible reason underlying this packing motif is that the distance between the approximately parallel planes of phenylene moieties of **33** is almost equivalent to the molecular distance of the hydrogen-bonded melamine dimer. From the viewpoint of crystal engineering, the use of cocrystallization to obtain new arrangements of aromatic layered structures is of great interest.

3. Behaviour of dynamic helical structures of multi-layered aromatic oligoureas in solution

3.1 Helical structures of oligo(*m*-phenylurea)s

Multi-layered oligo(*m*-phenylurea)s show well-ordered helical structure based on the all-*R* or all-*S* axis chirality of (*cis,cis*)-urea bonds (Figure 5b). In the crystals, both enantiomers exist in a 1:1 ratio,[6c] while in solution, the equilibrium between the enantiomers is rather fast, and the enantiomers cannot be distinguished even by ^{1}H NMR analyses in the presence of chiral reagents, such as (*R*)-binaphthol, at 183K.

3.2 Induction of handedness in helical oligo(*m*-phenylurea)s

Induction of handedness in helical oligomers is an important topic, because of the range of possible applications, including optical devices, chiral data storage, and chiral amplification. Several methodologies have been developed, for example, introducing optically active side chains into the helical backbone or adding chiral components that interact with the oligomer, but their effects strongly depend on the structures and features of the particular oligomers and even on the external environment.

Helical aromatic oligourea is a particularly desirable target for the induction of handedness because of its well-ordered stable conformations. Clayden et al and our group investigated the dynamic helical behaviours of helical oligo(*m*-phenylurea)s in solution by introducing chiral moieties at the terminus or at the central region.

3.2.1 Terminal chiral effect

Clayden et al examined the induction of handedness in oligoureas bearing a chiral sulfinyl or rotationally restricted amide group at the terminus by detecting the diastereotopic signals in ^{1}H NMR spectra.[11]

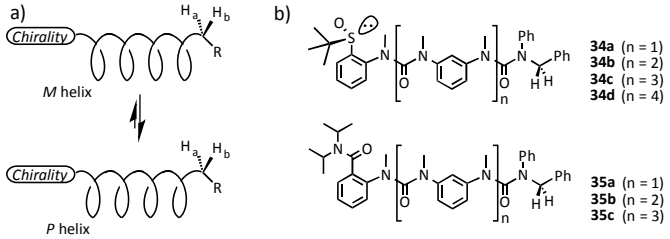

Figure 8. a) Schematic illustration of interconversion between the diastereomeric helices. b) Chemical structures of oligoureas bearing chiral *t*-butylsulfoxide group (**34a-d**) or amide group (**35a-c**).

In enantiomeric interconverting helices with a pair of terminal protons H_a and H_b (Figure 8a), the protons are rendered diastereotopic by the chirality of the helix. If either *M* or *P* helices predominates by virtue of the attached chiral moiety, or if the interconversion between *M* and *P* helices is slow, anisochronous signals of H_a and H_b could be observed in an AB system. Thus, ^{1}H NMR was used to investigate the chain length dependency of the helical handedness induced by groups at the terminus of the oligoureas. The target oligoureas possessed a chiral *t*-butylsulfoxide group (**34a-34d**) or a bulky amide group (**35a-35c**), which would prevent rapid helix inversion, at one terminus, and *N*-phenyl-*N*-benzyl urea as a diastereotopic probe at the other terminus (Figure 8b). The values of chemical shift difference (Δδ) between the two anisochronous signals of **34** and **35** are shown in Table 2. Anisochronicity clearly appeared in **34a-34c** and **35a-35b**, indicating that the influence of the chiral sulfinyl or bulky amide group could be transmitted up to 24 and 17 bond lengths, respectively. Loss of the helicity in longer oligomers was also supported by the results of CD analyses.

Table 2. Apparent diastereotopicity in the NCH_aH_bPh signals of oligoureas **34** and **35**

urea	NCH_aH_bPh signal	Δδ (ppb)
34a	AB system	80 (C_6D_6)
34b	AB system	83 ($CDCl_3$)
34c	AB system	10 ($CDCl_3$)
34d	2 H singlet	0 (various solvens)
35a	AB system	20 ($CDCl_3$)
35b	AB system	65 ($CDCl_3$)
35c	2 H singlet	0 (various solvens)

3.2.2 Central chiral effect

At the same time that Clayden et al were examining the induction of helical handedness of oligoureas by attachment of a terminal chiral moiety, we investigated the effect of chiral substituents at the central region of the oligoureas on the helical handedness, and identified the absolute helical structure based on empirical and theoretical studies of CD and vibrational CD (VCD) spectra.[12]

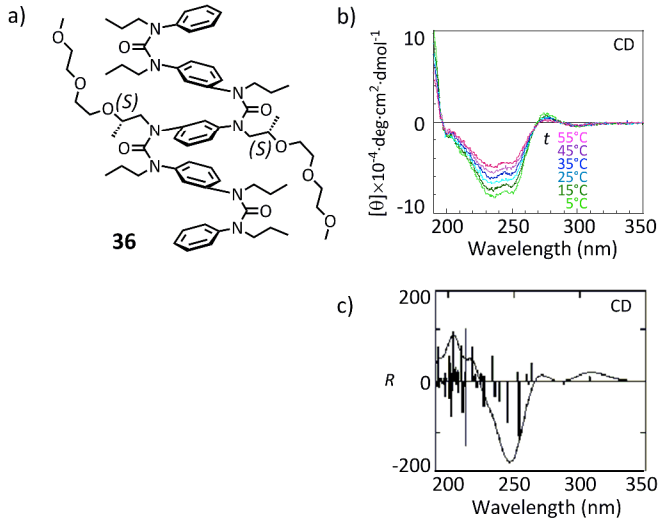

Figure 9. a) Chemical structure of tetra(*m*-phenylurea) (**36**). b) Experimental CD spectra of **36** in CH_3CN at various temperatures. c) Calculated (ZINDO) CD spectrum of tetra(*m*-phenylurea) (**5**) with all-*R* axis chirality.

We chose a 2-(methoxyethoxyethoxy)propyl group as a chiral substituent, not only to introduce chirality, but also to improve the solubility, and we introduced this group at the two central urea nitrogen atoms of tetra(*m*-phenylurea) to afford the

target oligourea **36** (Figure 9a). In the CD spectra, **36** bearing substituents with (*S*)-configuration showed a strong Cotton effect at 200-270 nm with high temperature-dependency, (the effect decreased with increasing temperature; Figure 9b), suggesting a bias of the helical handedness. To identify the absolute helical structure of **36**, the CD spectrum of tetra(*m*-phenylurea) **5** with all-*R* axis chirality was calculated by means of the semiempirical ZINDO method (Figure 9c). By comparison of the simulated CD data with experimental data, oligourea **36** bearing substituents with (*S*)-configuration could be identified as preferentially adopting helical structure with all-*R* axis chirality. This result was also supported by VCD analyses.

Although quantitative analysis of chiral induction in the helical oligoureas could not be achieved, CD analysis was found to be a useful detection method. Therefore, we next used it to examine the solvent dependency and the chain length dependency of the helical dynamic behavior of the oligoureas.

To analyze the conformations of oligoureas in various solvents by means of CD measurement, tetra(*m*-phenylurea) bearing hydrophilic substituents on every nitrogen atom (**37**) (Figure 10a) was prepared, and CD measurements were made in CH_3CN, CH_3OH, $CHCl_3$, and H_2O.[13] Figure 10b shows the temperature-dependency of CD intensity at 235 nm in each solvent. Similar dynamic behavior of the helicity was observed in all of the organic solvents, i.e., an increase of CD intensity with decreasing temperature, with only minor differences of the CD intensity, whereas a different result was obtained in H_2O. In H_2O, both the CD intensity and the temperature dependency were quite low, suggesting that the stability and the dynamicity of the helix were decreased in H_2O, possibly due to unfavorable interaction between the hydrophilic substituents of **37** and water molecules.

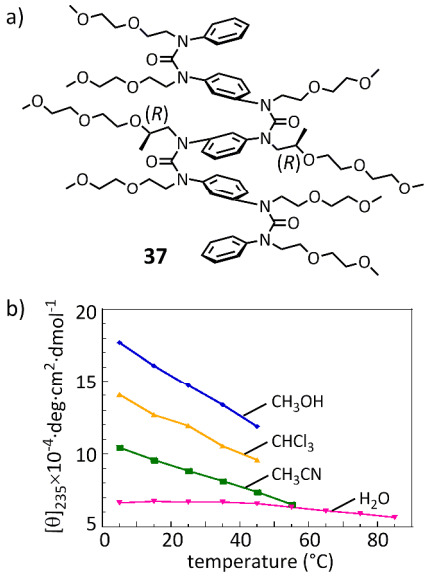

Figure 10. a) Chemical structure of tetra(*m*-phenylurea) (**37**). b) Temperature-dependency of CD intensity (235 nm) of **37** in various solvents.

The chain length dependency of the helical handedness induced by a chiral substituent in the central region is of interest for comparison with the results of Clayden et al, to understand the influence of the position of the chiral moiety in the oligoureas. The target oligo(*m*-phenylurea)s bearing one chiral hydrophilic *N*-substituents at the central urea bond (diurea **38**, tetraurea **39**, and hexaurea **40**) are shown in Figure 11a.[14] The normalized CD intensities of oligoureas of different chain lengths were almost the same (Figure 11b), though the spectral waveform of **38** is different from that of the other oligouras, probably because of a slight difference of conformation. The observation that **39** and **40** showed the same CD intensity means the chain length limit of the steric effect of a chiral *N*-substituent at the central position is the tetraurea, which is consistent with the results of Clayden et al. Therefore, the position of the chiral attachment would not be important in short oligoureas.

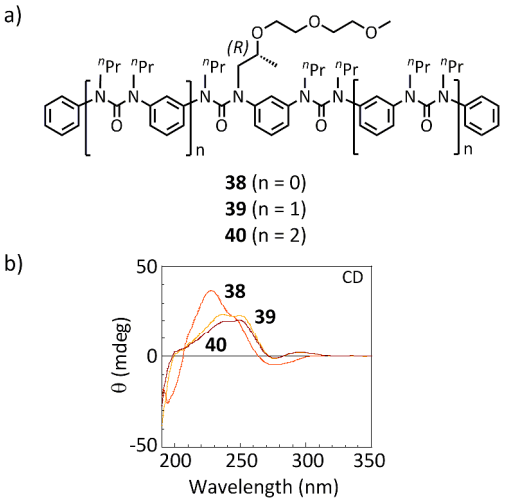

Figure 11. a) Chemical structures of oligoureas **38**-**40**. b) Normalized CD spectra of oligoureas **38**-**40** in CH_3CN at 25°C.

4. Biological Activity of multi-layered aromatic oligoguanidines

Multi-layered oligomeric foldamers have potential value for molecular recognition due to their well-ordered folded conformations that are both stable and flexible. Recently, derivative of **5** mimic host defence peptides in the antimicrobial behaviour.[15]

An interesting study of aromatic layered guanidines has shown that they bind sequence-specifically to the DNA minor groove.[16] Minor groove binders generally possess cationic functional groups, such as amidino or guanidino groups, at the terminal positions of the planar backbone, as represented by netropsin and distamycin, but the typical B-DNA minor groove, with a width of 5.7Å and a depth of 7.5Å, is large enough to accommodate rather bulkier compounds.

Multi-layered tetra(*p*-phenylguanidine) (**2**) and tetra(*m*-phenylguanidine) (**5**) (Figure 2 and 5) are of suitable size to fit the minor groove pocket, and their two cationic guanidino groups located on both sides of the layered phenyl groups are expected to interact with base pairs of DNAs. Figure 12 shows the result of a docking study of **2** and the duplex of dodecamer CGCGAATTCGCG, which suggests that **2** fits well at the 3'-(C)GAA(T)-5' region in the groove, with one cationic side near the base pairs. The DNA-binding ability of **2** and **5** was evaluated by ultrafiltration assay using calf thymus DNA (Table 3); these compounds showed high affinity, with binding constants (*Ka*) of 6.2×10^6 M^{-1} for **2** and 1.2×10^7 M^{-1} for **5**, which are higher than that of netropsin, a typical minor groove binder. The binding motifs of **2** and **5** with DNA were carefully examined by titration studies using CD and ^{1}H NMR spectroscopy, and the results were in agreement with those of

the computational model study. Further structural investigations should provide the basis for developing a new class of DNA groove binders.

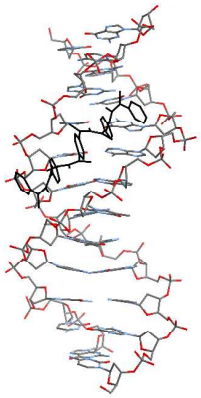

Figure 12. Calculated structure of the complex of **2** with the duplex of dodecamer CGCGAATTCGCG.

Table 3. Binding abilities of **2** and **5** with calf thymus DNA[a]

compound	*Ka* (M^{-1})	*n* (per base pair)
2	6.2 x 10^6	0.20
5	1.2 x 10^7	0.19
netropsin	1.0 x 10^5	0.52

[a] Binding constant (*Ka*) and number of binding sites per base pair (*n*) were calculated from Scatchard analyses of ultrafiltration assay data.

Conclusions

In this focus, we have presented an overview of the structural properties of aromatic oligoureas and oligoguanidines. Cis conformational properties of *N,N'*-dialkylated urea and guanidine are useful and reliable building blocks for aromatic multilayers. Among them, the compounds with axial chilarity showed dynamic helical properties. Efficient synthetic method of aromatic oligoureas has been reported, while there is still difficulty in the synthesis of oligoguanidines, and there is no report about the related oligothioureas. Since the folding structures of aromatic oligoureas and oligoguanidines depend on cis conformational properties of *N,N'*-dialkylated urea and guanidine, and need no covalent linkers nor rigid interactions such as hydrogen bonding and metal coordination. Therefore, aromatic multilayered and helical oligoureas and oligoguanidines are potentially useful as backbone structures of novel functional foldamers, including electronic devices, chiral recognition, and bioactive substances.

Notes and references

Department of Chemistry, Faculty of Science, Ochanomizu University, 2-1-1 Otsuka, Bunkyo-ku, Tokyo 112-8610, Japan.

1 G. Guichard and I. Huc, *Chem. Commun.*, 2011, **47**, 5933.

2 (a) S. Breidenbach, S. Ohren, M. Nieger and F. Vögtle, *J. Chem. Soc., Chem. Commun.*, 1995, 1237; (b) R. S. Lokey and B. L. Iverson, *Nature*, 1995, **375**, 303; (c) P. N. W. Baxter, J. –M. Lehn, G. Baum and D. Fenske, *Chem. Eur. J.*, 2000, **6**, 4510.

3 (a) H. Kagechika, T. Himi, E. Kawachi, Y. Hashimoto and K. Shudo, *J. Med. Chem.,* 1989, **32**, 2292; (b) A. Itai, Y. Toriumi, N. Tomioka, H. Kagechika, I. Azumaya and K. Shudo, *Tetrahedron Lett.*, 1989, **30**, 6177; (c) A. Tanatani, K. Yamaguchi, I. Azumaya, R. Fukutomi, K. Shudo and H. Kagechika, *J. Am. Chem. Soc.*, 1998, **120**, 6433.

4 (a) N. Fujimoto, M. Matsumura, I. Azumaya, S. Nishiyama, H. Masu, H. Kagechika, A. Tanatani, *Chem. Commun.* 2012, **48**, 4809; (b) I. Okamoto, Y. Takahashi, M. Sawamura, M. Matsumura, H. Masu, K. Katagiri, I. Azumaya, M. Nishino, Y. Kohama, N. Morita, O. Tamura, H. Kagechika, A. Tanatani, *Tetrahedron* 2012, **68**, 5346; (c) M. Kanai, T. Hirano, I. Azumaya I. Okamoto H. Kagechika A. Tanatani, *Tetrahedron*, 2012, **68**, 2778; (d) M. Matsumura, A. Tanatani, T. Kaneko, I. Azumaya, H. Masu, D. Hashizume, H. Kagechika, A. Muranaka, M. Uchiyama, *Tetrahedron* 2013, **69**, 10927.

5 A. Tanatani, A. Yokoyama, I. Azumaya, Y. Takakura, C. Mitsui, M. Shiro, M. Uchiyama, A. Muranaka, N. Kobayashi and T. Yokozawa, *J. Am. Chem. Soc.*, 2005, **127**, 8553.

6 (a) K. Yamaguchi, G. Matsumura, H. Kagechika, I. Azumaya, Y. Ito, A. Itai and K. Shudo, *J. Am. Chem. Soc.*, 1991, **113**, 5474; (b) A. Tanatani, H. Kagechika, I. Azumaya, K. Yamaguchi and K. Shudo, *Chem. Pharm. Bull.*, 1996, **44**, 1135; (c) A. Tanatani, H. Kagechika, I. Azumaya, R. Fukutomi, Y. Ito, K. Yamaguchi and K. Shudo, *Tetrahedron Lett.*, 1997, **38**, 4425; (d) M. Matsumura, A. Tanatani, I. Azumaya, H. Masu, D. Hashizume, H. Kagechika, A. Muranaka, M. Uchiyama, *Chem. Commun.* 2013, **49**, 2290.

7 F. C. Krebs and M. Jørgensen, *J. Org. Chem.*, 2002, **67**, 7511.

8 F. D. Lewis, G. B. Delos Santos and W. Liu, *J. Org. Chem.* 2002, **67**, 7511.

9 J. Clayden, L. Lemiègre and M. Helliwell, *J. Org. Chem.*, 2007, **72**, 2302.

10 S. Kohmoto, S. Sekizawa, S. Hisamatsu, H. Masu, M. Takahashi and K. Kishikawa, *Cryst. Growth Des.*, 2014, **14**, 2209.

11 J. Clayden, L. Lemiègre, G. A. Morris, M. Pickworth, T. J. Snape and L. H. Jones, *J. Am. Chem. Soc.* 2008, **130**, 15193.

12 M. Kudo, T. Hanashima, A. Muranaka, H. Sato, M. Uchiyama, I. Azumaya, T. Hirano, H. Kagechika and A. Tanatani, *J. Org. Chem.* 2009, **74**, 8154.

13 M. Kudo, I. Azumaya, H. Kagechika and A. Tanatani, *Chirality*, 2011, **1E**, E80.

14 M. Kudo, K. Katagiri, I. Azumaya, H. Kagechika and A. Tanatani, *Tetrahedron*, 2012, **68**, 4455.

15 S. R. Dennison, D. A. Phoenix, T. J. Snape, *Bioorg. Med. Chem. Lett.* 2013, **23**, 2518.

16 R. Fukutomi, A. Tanatani, H. Kakuta, N. Tomioka, A. Itati, Y. Hashimoto, K. Shudo and H. Kagechika, *Tetrahedron Lett.* 1998, **39**, 6475.